ELSEVIER

Marine Geology 176 (2001) 139–156

MARINE GEOLOGY
INTERNATIONAL JOURNAL OF MARINE GEOLOGY, GEOCHEMISTRY AND GEOPHYSICS

www.elsevier.nl/locate/margeo

The role of swash infiltration in determining the beachface gradient: a numerical study

Gerhard Masselink[a,*], Ling Li[b]

[a]*Department of Geography, Loughborough University, Loughborough LE11 3TU, UK*
[b]*School of Civil and Environmental Engineering, Contaminated Land Assessment and Remediation Research Centre, The University of Edinburgh, Edinburgh EH9 3JN, UK*

Received 6 October 2000; accepted 23 March 2001

On sand and gravel beaches, the increase of the gradient of the beachface with increasing sediment size has been attributed to swash infiltration. The present study uses a process-based numerical model to examine in detail the role of swash infiltration in determining the beachface gradient. It is found that swash infiltration increases the onshore asymmetry in the swash flow, thereby enhancing onshore sediment transport and resulting in relatively steep beachface gradients. However, the accretionary effects of swash infiltration are only evident when the rate of infiltration is sufficiently large, i.e. when the total infiltration volume over a wave cycle exceeds c. 2% of the uprush volume. This threshold is attained when the hydraulic conductivity exceeds 1 cm/s which is approximately equivalent to a grain size coarser than 1.5 mm. This finding suggests that the correlation between beachface gradient and sediment size observed on sandy beaches is not due to enhanced swash asymmetry caused by swash infiltration. For gravel beaches, however, swash infiltration is likely to be the dominant factor in controlling the beachface gradient with increased hydraulic conductivity (i.e. sediment size) resulting in steeper beachface gradients.

Keywords: beachface; swash zone; sediment transport; numerical modelling

The beachface is the sloping section of the beach profile below the berm normally exposed to the action of wave swash. The shape of the beachface ranges from planar to concave, although under conditions of profile adjustment the beachface may have a convex shape (Sonu and van Beek, 1971; Sonu and James, 1973; Makaske and Augustinus, 1998). The most characteristic feature of the beachface is its steep gradient compared to the rest of the beach profile. This is generally ascribed to the asymmetry in the swash flow due to swash infiltration into the beachface and frictional drag on the swash (Bagnold, 1940). The term 'swash infiltration' in this context refers to the net infiltration that occurs during swash motion.

The effect of swash infiltration on sediment transport in the swash zone and beachface morphology has been known for quite some time (Grant, 1948) and is conceptually easy to comprehend. Swash infiltration weakens the backwash with respect to the uprush because most of the water that infiltrates will not participate in the backwash (Kemp, 1975). The ensuing

* Corresponding author. Fax: +44-1509-223930.
E-mail addresses: g.masselink@lboro.ac.uk (G. Masselink), ling.li@ed.ac.uk (L. Li).

0025-3227/01/$ - see front matter
PII: S0025-3227(01)00161-X

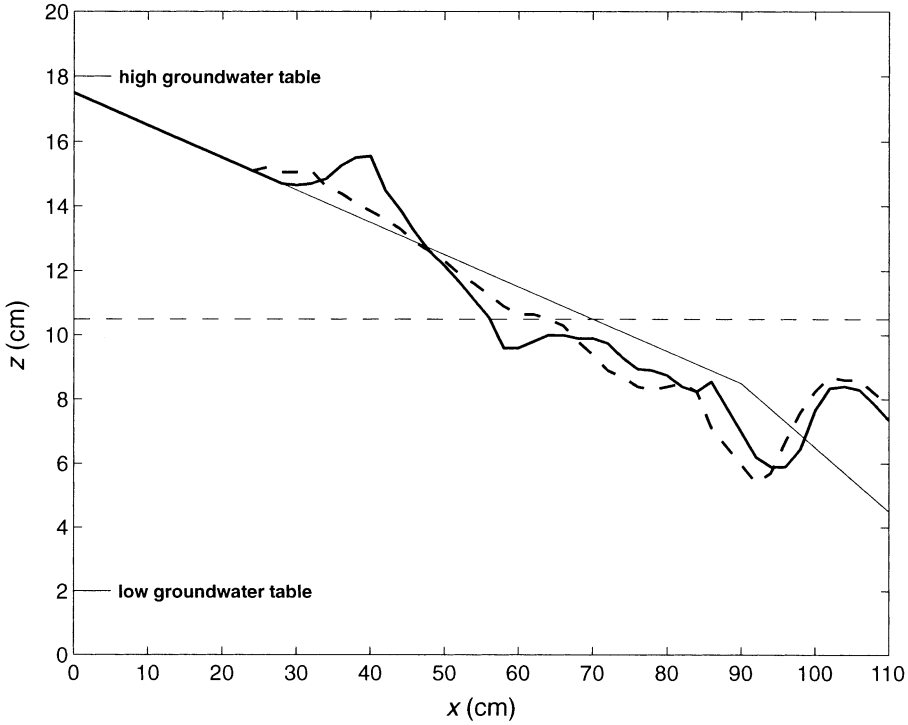

Fig. 1. Results of a small-scale laboratory experiment whereby a sandy beach was subjected to mildly erosive wave conditions with an artificially elevated beach groundwater table (inhibiting swash infiltration; solid line) and a artificially lowered beach groundwater table (promoting swash infiltration; dashed line). In both cases, the shoreline retreated and berm/bar morphology developed. However, the size of the berm and the gradient of the beachface were substantially larger for the experimental run with the lowered beach groundwater table. Clearly, swash infiltration, enhanced by lowering of the beach groundwater table, promotes onshore sediment transport and results in the formation of a beach with a pronounced berm and a steep beachface gradient (unpublished data).

swash asymmetry enhances onshore sediment transport and a steepening of the beachface until a gradient is attained whereby the onshore force due to swash asymmetry is balanced by the offshore gravity component. The resulting gradient, referred to as the equilibrium beachface gradient, increases with the amount of swash infiltration (Quick, 1991). Swash infiltration, and hence onshore sediment transport in the swash zone, can be promoted by artificially lowering the beach groundwater table (Fig. 1). Coastal engineers apply this method, known as beach dewatering, on eroding beaches with the objective to increase swash infiltration and promote onshore sediment transport (for a review of the beach dewatering technique, see Turner and Leatherman, 1997).

On tidal beaches, swash infiltration depends largely on the tidal stage with infiltration predominantly occurring during the rising tide when the beach is relatively dry (Turner, 1993). However, if tidal action is ignored, the amount of water infiltrating into the beach during swash action depends primarily on the hydraulic conductivity (or permeability) of the beachface. The permeability of the beachface increases with sediment size and to a lesser degree with sediment sorting (Krumbein and Monk, 1942). Hence, the well-known finding that beachface gradient increases with sediment size and sorting (e.g. Bascom, 1951; Shepard, 1963; McLean and Kirk, 1969) is often explained in terms of beachface permeability and swash infiltration.

There are some indications in the literature that suggest that swash infiltration is only important in controlling the beachface gradient when the beach sediment is relatively coarse. Bagnold (1940) conducted a series of laboratory experiments to investigate the relationship between sediment size, swash

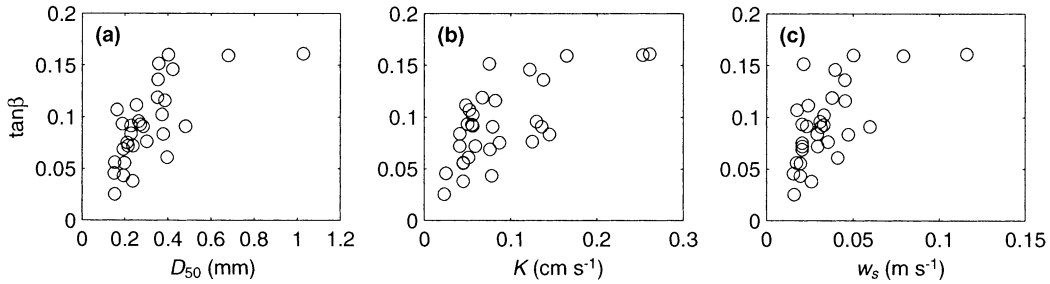

Fig. 2. Scatter diagrams of beach gradient tan β versus: (a) sediment size D_{50}; (b) permeability K; and (c) sediment fall velocity w_s for thirty one low-energy beaches in south-western Australia. All sediment properties have been determined independently: D_{50} was obtained using sieving, K was measured in situ at the top of the beach using a constant head method and w_s was determined using a settling tube. The sediment samples for D_{50} and w_s were obtained from the mid-beachface position. (Data from Hegge, 1994).

infiltration and beach gradient. For $D_{50} = 3$ mm, it was found that swash infiltration is significant and results in the formation of a relatively steep and concave-upward beachface. The larger the sediment size, the greater the amount of swash infiltration and the steeper the beach. For $D_{50} = 0.5$ mm, however, Bagnold (1940) concluded that swash infiltration is negligible suggesting that a beach composed of such sediments is virtually impermeable. Unfortunately, no experiments were conducted for intermediate sediment sizes to indicate at what sediment size swash infiltration starts playing a significant role.

Field observations also suggest that for relatively fine sediments swash infiltration does not play an important role in controlling the beachface gradient. Dubois (1972) measured beachface gradients on fine to medium sand beaches enriched in heavy minerals along the shores of Lake Michigan. The data showed that small, but heavy sand grains ($D_{50} \approx 0.2$ mm) formed steeper beachfaces than large, but light sand grains ($D_{50} \approx 0.4$ mm), indicating that permeability was not a significant factor in controlling the beachface gradient. The results displayed a strong positive correlation between the beachface gradient and the percentage of heavy minerals in the sediment. It was hypothesized that the correlation was due to a dependence of the equilibrium beachface gradient on sediment fall velocity, which was mainly a function of the sediment density at the study site (but generally depends on sediment size). Such dependence suggests that the beachface gradient can also be controlled by suspended sediment transport processes as envisioned in the heuristic model of Dean (1973). According to this model, the heavier a sediment particle, the greater its resistance to removal by the backwash and hence the steeper the equilibrium gradient is.

It thus appears that there are (at least) two explanations for the dependence of beachface gradient on sediment size found in nature as indicated by Komar (1998). On beaches consisting of relatively fine sediments, the beachface gradient is established mainly by cross-shore transport of suspended sediments. In this case, the beachface gradient will increase in a direct proportion with the ability of the sediments to resist transport (Dubois, 1972) and will increase with the sediment fall velocity (a function of the size and density of sediment particles). On beaches with relatively coarse sediments, the asymmetry in the swash flow resulting from swash infiltration is more important and the gradient of the beachface will increase with the permeability of the beach sediment (a function of size and sorting of sediment particles). In reality, correlation between beachface gradient and sediment properties (e.g. Dalrymple and Thompson, 1976; Sunamura, 1984) cannot be used to identify the most important process controlling the gradient because sediment size, permeability and fall velocity are highly interrelated. When the beachface gradient is plotted versus each of the three sediment characteristic parameters (Fig. 2), similar trends are observed, providing no discrimination against either the mechanism based on the sediment permeability or the hypothesis built on the sediment fall velocity.

The critical grain size above which infiltration effects start to play a dominant role in controlling the beachface gradient is not known, although from

the work of Bagnold (1940), it can be deduced that it is likely to exceed 0.5 mm. Knowledge of this threshold is of great use from a numerical modeling point of view. Models of shoreline evolution have so far made slow progress in dealing with the swash zone (Butt and Russell, 2000). To a large extent this can be ascribed to the complexities involved with sediment transport processes in the swash zone. In particular, the role of interactions between the swash flow and the beach groundwater are still poorly understood, despite some recent studies (Baird et al., 1996; Turner and Masselink, 1998; Li and Barry, 2000; Butt and Russell, 2000; Butt et al., 2001). If it can be assessed under what conditions groundwater effects are insignificant this would significantly simplify the approaches to model sediment transport processes in the swash zone.

The main objective of this paper is therefore to investigate when (i.e. for what sediment size) swash infiltration becomes important in controlling the beachface morphology. It is appropriate to point out that the present study focuses on swash asymmetry induced/enhanced by infiltration (i.e. swash infiltration losses). This study does not address the effects of vertical flow through a porous bed resulting in either seepage forces changing the effective weight of surficial sediments, or boundary layer, 'thinning' and 'thickening' due to infiltration and exfiltration, respectively (cf. Turner and Masselink, 1998). A process-based numerical model is used here to investigate the role of swash infiltration on swash zone sediment transport. The model is able to determine the effect of swash infiltration on swash hydrodynamics, and hence sediment transport, but does not account for sediment suspension. Therefore, the model enables an investigation of the role of swash infiltration on beachface morphology without the confounding effects of sediment suspension. The outline of this paper is as follows. Section 2 discusses the sediment transport mechanism implemented in the numerical model. Section 3 gives a brief description of the numerical model and investigates the effect of swash infiltration on swash hydrodynamics under different incident wave conditions. The model is then used to simulate swash zone morphological changes affected by infiltration in Section 4. The results are subsequently discussed in Section 5, followed by conclusions in Section 6.

One of the simplest approaches to model sediment transport is the energetics-based model of Bagnold (1963, 1966) modified by Hardisty (1984) for use in the swash zone:

$$I_u = \frac{k_u u_u^3 T_u}{\tan\phi + \tan\beta}, \tag{1}$$

$$I_b = \frac{k_b u_b^3 T_b}{\tan\phi - \tan\beta}, \tag{2}$$

where I is the immersed weight sediment transport load per unit m width; k is a calibration coefficient; u represents a statistical measure of the flow velocity; T is the flow duration; ϕ is the friction angle of the sediment ($\tan\phi = 0.625$); β is the beach angle; and the subscripts 'u' and 'b' refer to the uprush and backwash stages of the swash flow, respectively. According to the Bagnold model, sediment transport during the uprush is inhibited by the beach gradient (sand is moved up-slope), whereas the beach gradient promotes sediment transport during the backwash (sand is moved down-slope). The mean swash velocity is commonly entered into Eqs. (1) and (2) (Hardisty, 1984; Jago and Hardisty, 1984; Hughes et al., 1997). However, because sediment transport is considered proportional to the velocity cubed, the cube-root mean cubed velocity (obtained by taking the cube root of the mean cubed velocities) is more appropriate (Masselink and Hughes, 1998).

The Bagnold model provides a suitable framework for relating swash zone hydrodynamics to sediment transport and morphological changes because it enables a definition of the equilibrium bed gradient (when $I_u = I_b$):

$$\tan\beta = \tan\phi \frac{F-1}{F+1}, \tag{3}$$

where

$$F = \frac{k_u u_u^3 T_u}{k_b u_b^3 T_b}, \tag{4}$$

Eq. (3) suggests that F must be larger than 1 for a positive beachface gradient to be maintained and that the equilibrium gradient increases with F. Jago

Table 1
Results of least-squares analysis using the cube-root mean cubed flow velocity (tan β = beachface gradient; D_{50} = mid-beachface sediment size in mm; N = number of swash events; k_u = k-coefficient for the uprush; k_b = k-coefficient for the backwash; the confidence interval is 95%; r^2 = coefficient of determination; data from Edwards (1997) and Masselink and Hughes (1998))

Location	tan β	D_{50}	Uprush				Backwash			
			N	k_u	95%	r^2	N	k_b	95%	r^2
Trigg	0.12	0.6	30	19.9	3.0	0.50	30	9.4	1.2	0.76
Myalup	0.14	0.5	27	14.5	2.5	0.58	27	7.4	1.1	0.72
Brighton	0.20	0.7	22	17.8	2.2	0.70	16	15.3	2.5	0.45
City	0.22	0.8	19	17.0	3.3	0.46	21	7.8	1.5	0.48
All			98	16.1	1.3	0.57	94	8.0	0.7	0.64

and Hardisty (1984) assumed that $k_u = k_b$ and $u_u T_u = u_b T_b$, so that F reduces to $(u_u/u_b)^2$, which is simply a measure of the swash velocity asymmetry.

Strictly speaking, Eqs. (1) and (2) only apply to sediment transport by bedload, but Hughes et al. (1997) and Masselink and Hughes (1998) calibrated the Bagnold model for the swash zone by relating the total sediment load carried up and down the beachface to uprush and backwash flow characteristics. They justified their approach by arguing that: (1) sediment transport in the swash zone on natural beaches occurs predominantly under sheet flow conditions; and (2) sheet flow is similar to bedload in the sense that in both cases the sediment transport rate depends on the flow velocity cubed (Wilson, 1987; Ribberink and Al Salem, 1990; Nielsen, 1992).

Masselink and Hughes (1998) measured near-bed swash flow velocities and total sediment load during wave uprush and backwash of twenty seven swash events. Calibration of the Bagnold model (Eqs. (1) and (2)) indicated different constants of proportionality (k-values) for wave uprush and backwash, with the uprush value being approximately twice that obtained for the backwash. In other words, given the same flow velocity and flow period, the uprush would move twice the amount of sediment up-slope than the backwash would move down-slope. Masselink and Hughes (1998) provide three explanations why the uprush

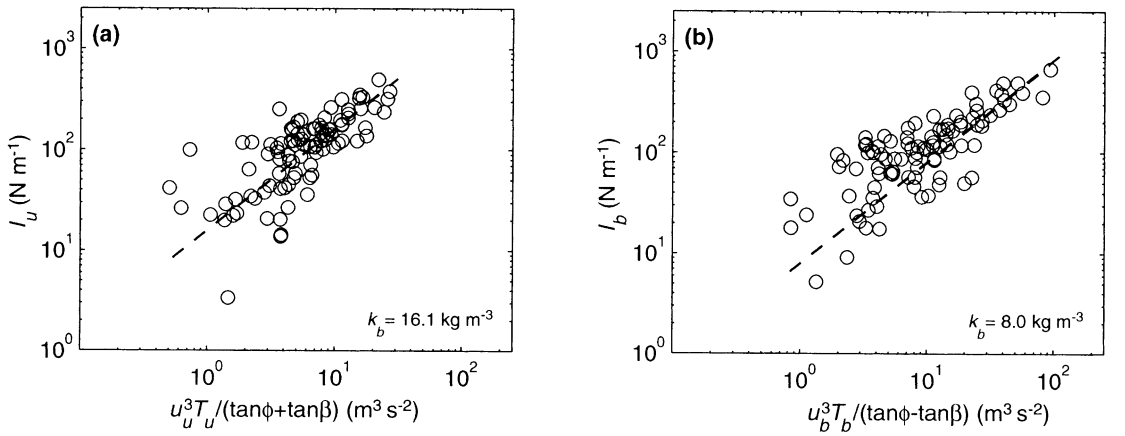

Fig. 3. Calibration of the Bagnold model (Eqs. (1) and (2)) for sediment transport in the swash zone during: (a) uprush; and (b) backwash. Data from Edwards (1997) and Masselink and Hughes (1998).

appears to be more 'effective' than the backwash in transporting sediment. First, wave uprush is characterized by decelerating flows of shorter duration and larger magnitude than the accelerating backwash. This results in a thinner boundary layer and hence larger bed shear stresses during the uprush (King, 1991; Nielsen, 1992). Second, sediment mobilized by wave breaking and/or bore collapse at the initiation of wave uprush will be added to the sediment entrained by the instantaneous uprush flow. Third, vertical flow through the beachface (instantaneous in-exfiltration) may promote uprush sediment transport (Turner and Masselink, 1998) due to its effect on the thickness of the boundary layer (Conley and Inman, 1994).

If sediment transport in the swash zone is modeled using Bagnold's energetics approach the resulting equilibrium gradient is strongly dependent on the ratio k_u/k_b (Eqs. (3) and (4)). It is therefore appropriate to determine whether the results of Masselink and Hughes (1998), which were obtained on a single beach, are comparable with other beaches. In particular, the possible dependence of the k-values on beachface gradient and sediment characteristics warrants further investigation. To this effect, Edwards (1997) conducted three additional field experiments using the same methodology as Masselink and Hughes (1998). The four data sets on swash zone sediment transport were used to calibrate Eqs. (1) and (2) (Table 1). Apart from the backwash data collected on one of the beaches (Brighton) there is excellent agreement between the k-values obtained from the different data sets despite the range in beach gradient present in the data ($\tan\beta = 0.12$–0.22). Calibration of the complete data set (Fig. 3) resulted in $k_u = 16.1 \pm 1.3$ kg/m^3 ($r^2 = 0.57$) and $k_b = 8.0 \pm 0.7$ kg/m^3 ($r^2 = 0.64$), confirming the original finding of Masselink and Hughes (1998) that $k_u \approx 2k_b$. In a recent study Puleo et al. (2000) used the suspended load sediment transport model of Bagnold (1963, 1966), which is very similar to Eqs. (1) and (2), to compare against measured suspended transport rates in the swash zone. They also found that $k_u \approx 2K_b$ (their Figs. 12 and 13).

The effects of swash infiltration on swash zone hydrodynamics, sediment transport and beach profile changes were investigated using a process-based numerical model that simulates interacting surface and subsurface flow and sediment transport processes. The details of the model have been given elsewhere (Li and Barry, 2000; Li et al., 2001). Here only the model formulation and assumptions are described briefly.

In the model, the transformation of monochromatic waves across the nearshore zone and the motion of swash are modeled using the non-linear shallow water equations (SWE; Peregrine, 1972). The SWE assume that the fluid velocities are uniform in the vertical direction, hence changes in the bottom boundary layer due to flow acceleration/deceleration (King, 1991; Nielsen, 1992) and swash infiltration/exfiltration (Conley and Inman, 1994) are not accounted for. The role of turbulent bore dissipation (Puleo et al., 2000) is not directly considered in the model either. Modifications of the SWE are made to account for the mass and momentum exchange between sea water and beach groundwater due to in-exfiltration. Bottom friction is also included by using the quadratic approximation, $1/2f|u|u$, where f is a friction factor and u is the flow velocity (Packwood and Peregrine, 1981). A value of $f = 0.015$ was assumed (Kobayashi et al., 1989). Only the saturated beach groundwater flow, as governed by the Laplace equation, is considered in the model. However, the capillary effects on the saturated flow are incorporated through the free-surface boundary condition at the water table (Parlange and Brutsaert, 1987; Li et al., 1997). The wave model is coupled with the groundwater flow model via the boundary conditions at the beach. For the groundwater flow, the seaward boundary conditions are determined by the shoreline position and the local sea surface elevation, both of which are calculated by the wave motion model. The rates of in-exfiltration across the beach computed by the groundwater flow model are then inputted to the wave model. The instantaneous sediment transport rate I_i is calculated at each cross-shore grid point based on the Bagnold model according to

$$I_{i,u} = \frac{k_u u_{i,u}^3}{\tan\phi + \tan\beta}, \tag{5}$$

$$I_{i,b} = \frac{k_b u_{i,b}^3}{\tan\phi + \tan\beta}, \tag{6}$$

where $u_{i,u}$ and $u_{i,b}$ are the instantaneous flow velocities derived from the wave motion model and $k_u = 2k_b$. Strictly speaking, Eqs. (5) and (6) have been formulated for bedload transport only, as discussed above. However, validation of the bedload equations by Masselink and Hughes (1998) using total load measurements gives sufficient confidence to use the formulations in the present model to predict total load sediment transport (bedload and suspended load). It should be noted that at present no other sediment transport model for use in the swash zone is readily available. The sum of the instantaneous rates over a wave cycle gives the net sediment transport rate, which is used to predict the beach profile changes based on the continuity equation. The location of the nodes at the beachface in the groundwater flow model, and the local beach slope in the wave motion model and the sediment transport model are then adjusted according to the beach deformation.

For the present purpose, the model domain comprises of a sand/gravel beach with an initially constant slope ($\tan\beta = 0.15$) starting at a depth of 3 m. At the seaward boundary, the wave model is forced by a monochromatic incoming wave field characterized by a wave height H and period T. The beach groundwater dynamics depend largely on the hydraulic conductivity or permeability K of the beach sediment. Various empirical formulations are available for estimating K from sediment characteristics (Krumbein and Monk, 1942; Bear, 1972), however, different formulations can give estimates that may differ by one order of magnitude (Butt et al., 2001). Therefore, rather than specifying a sediment size in the model it was considered more appropriate to use the hydraulic conductivity K. As a reference, sand and gravel are characterized by hydraulic conductivity ranges of 0.01–1 and 1–10 cm/s, respectively.

In the model, a small non-dimensional water depth is used in defining the instantaneous shoreline. One problem with the numerical simulation of swash motion on relatively impermeable beaches ($K < 1$ cm/s) is that the beachface during the backwash remains covered by a thin lens of slowly moving water. On permeable beaches ($K > 1$ cm/s) this problem does not occur because infiltration during the backwash 'clears' the beachface very effectively. The thickness of this backwash lens is very small with most of it being less than 2 mm. As a result, the downrush limit (i.e. the lowest point within the swash zone that falls dry) is elevated significantly above the still water level, and the swash length (i.e. the distance between uprush and downrush limit) is relatively small. To overcome this problem, a critical water depth h_{c1} of 2 mm was used to distinguish between 'wet' and 'dry' in analyzing the simulation results. It should be noted that the selection of h_{c1} only affects the definition of the apparent swash excursion when analyzing the simulation results for relatively impermeable beaches (results for permeable beaches are not significantly affected). The swash excursion decreases and the backwash period increases with decreasing h_{c1}. However, swash velocities are not affected by h_{c1}. It is questionable whether such shallow flows (2 mm deep) are capable of transporting sediments. Visual field observations suggest that sediment transport at the end of the backwash under very shallow water depths ($h < 1$ cm) is limited. For this reason a second critical water depth h_{c2} was formulated defining the minimum depth required for sediment transport to occur. No observational data are available to give insight into the character of very shallow backwash flows, therefore h_{c2} was intuitively set to 1 cm. The model output is sensitive to h_{c2} with small values promoting backwash sediment transport because it allows for extended backwash events. However, sensitivity of the morphological results to h_{c2} is only evident for simulations with relatively low permeabilities ($K < 1$ cm/s).

Validation of the groundwater/swash part of the numerical model using analytical solutions is presented in Li and Barry (2000). These validations indicate that the model adequately reproduces: (1) a steady state groundwater circulation from the upper part of the beach to the lower part (Longuet-Higgins, 1983); and (2) the periodic local groundwater circulation that occurs below progressive bores (Packwood and Peregrine, 1979) and wave swash (Turner and Masselink, 1998). The sediment transport part of the model has not been validated. Such validation would require phase-resolving (within the swash cycle) data of swash hydrodynamics, infiltration/exfiltration, sediment transport loads and beach profile changes, however, these data are currently not available. The model is used here as a tool to investigate the importance of infiltration losses on sediment transport processes in the swash zone and is not intended to be a complete model for beachface development.

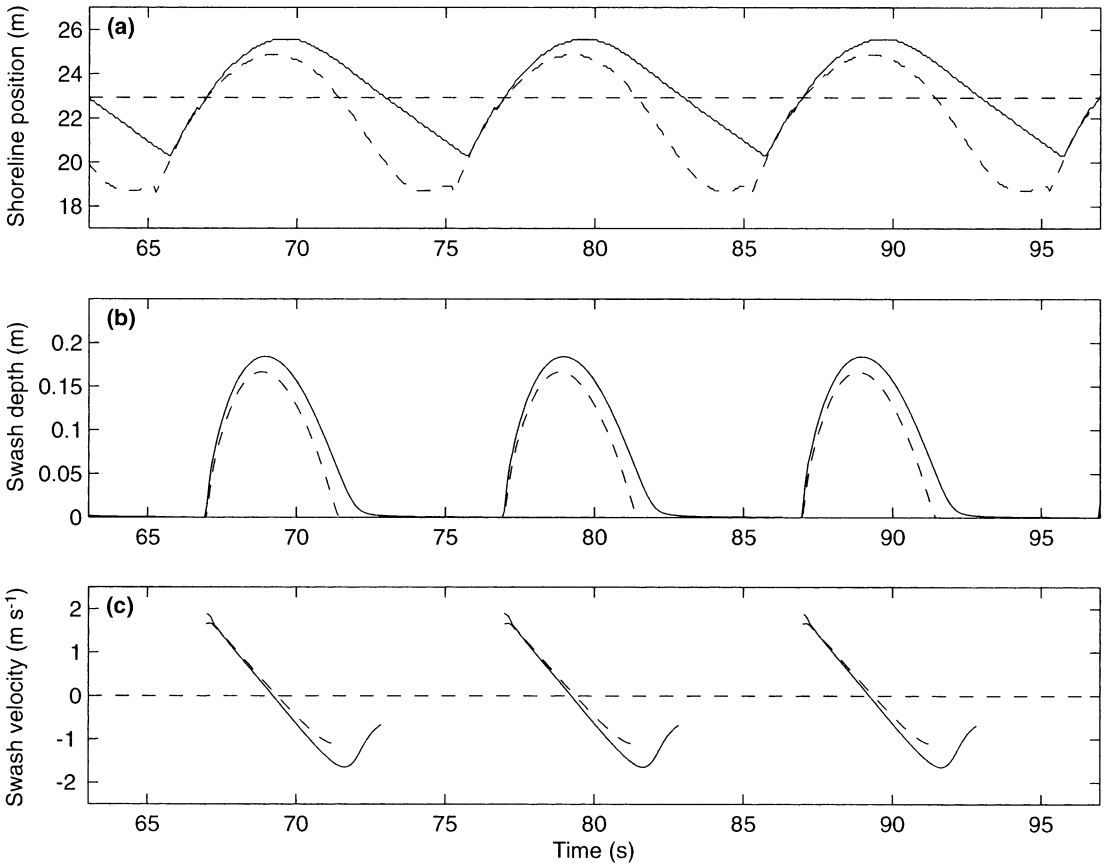

Fig. 4. Simulated time series of: (a) position of the instantaneous shoreline position; (b) swash depth; and (c) swash velocity. Model input conditions were tan $\beta = 0.15$, $H = 0.4$ m, $T = 10$ s and $K = 10$ cm/s. The model was run with (dashed lines) and without (solid lines) groundwater effects. Swash depth and swash velocity were computed at the mid-swash position of the model run without groundwater effects, indicated by the dashed horizontal line in (a). The intersection of the still water level with the beachface is located at $x = 20$ m in (a).

This section will focus on the effects of infiltration on swash zone hydrodynamics. All simulations discussed in this section were conducted assuming a rigid beach (sediment transport and beach profile changes are not included).

The first two numerical simulations were conducted with and without groundwater effects. Both simulations used the same initial beach slope and wave conditions (tan $\beta = 0.15$, $H = 0.4$ m and $T = 10$ s). For the simulation with groundwater effects, a highly permeable beach ($K = 10$ cm/s; equivalent to coarse gravel) was used. The results show that the effect of infiltration on the uprush phase of the swash flow is limited. Only a moderate reduction in the runup limit and the swash depth can be observed (Fig. 4a, b), and there is no discernable effect of infiltration on the uprush flow velocities nor on the duration of the uprush (Fig. 4c, b). In contrast, the effect of infiltration is significant on the backwash phase of the flow. If groundwater effects are ignored, a thin lens of water remains present over most of the lower part of the beachface during the latter stages of the backwash. The landward extent of this lens of water (i.e. the instantaneous shoreline) moves down the beachface at a relatively slow rate and is encountered by the proceeding wave at a location quite high on the beachface. As a result, the downrush limit (defined as the lowest part on the beachface that is periodically

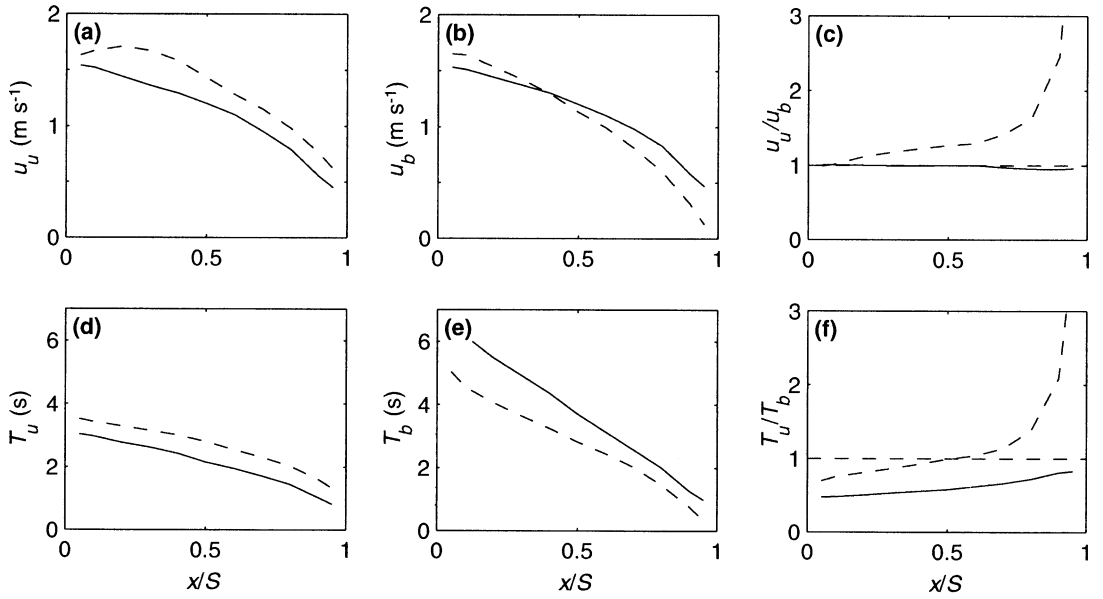

Fig. 5. Simulated cross-shore variation in swash zone parameters: (a) mean uprush velocity u_u; (b) mean backwash velocity u_b; (c) velocity asymmetry u_u/u_b; (d) uprush period T_u; (e) backwash period T_b; and (f) time asymmetry T_u/T_b. Model input conditions were $\tan\beta = 0.15$, $H = 0.4$ m, $T = 10$ s and $K = 10$ cm/s. The model was run with (dashed lines) and without (solid lines) groundwater effects. The cross-shore location is expressed as the relative swash zone position x/S, where x is the distance landward of the downrush limit and S is the swash length.

exposed during swash action) is elevated with respect to still water level (Fig. 4a). When groundwater effects are included, however, most of the beachface is cleared of water prior to the arrival of the proceeding wave due to infiltration. Consequently, the downrush limit coincides with or falls below the intersection of the still water level with the beachface (Fig. 4a), thereby significantly increasing the horizontal extent of the swash motion (swash length S). Infiltration also results in a reduction of the flow depths and velocities during the backwash (Fig. 4b and c). Most importantly, the duration of the backwash is significantly reduced due to infiltration.

The cross-shore variation in swash flow characteristics was also investigated for the two simulations discussed above (Fig. 5). Uprush/backwash velocities and periods display a progressive decrease from the downrush to the runup limit (Fig. 5a,b,d and e). The significance of swash infiltration becomes apparent when the velocity and time asymmetry of the swash flow (u_u/u_b and T_u/T_b, respectively) are investigated. When groundwater effects are not considered, u_u/u_b is close to 1 over the entire swash zone, whereas T_u/T_b progressively increases from 0.5 to 1 in the landward direction (Fig. 5c and f). Thus, uprush and backwash velocities are comparable, but the uprush is significantly shorter than the backwash everywhere in the swash zone. In order to conserve mass, this must imply that the uprush flow is significantly deeper than the backwash. When groundwater effects are considered, the reduction in the backwash velocity causes a significant increase in u_u/u_b. In addition, T_u/T_b exceeds unity in the upper part of the swash zone indicating that the uprush period is longer than the backwash period. It can be inferred that swash infiltration enhances onshore flow asymmetry and promotes the development of onshore time asymmetry. Both factors are expected to promote onshore sediment transport.

Subsequently, a large number of model runs were carried out to investigate the dependence of swash hydrodynamics on the incident wave conditions, beach gradient and groundwater effects. Model runs were carried out by changing the input parameters $\tan\beta$ (0.075–0.25 in 0.025 increments), H (0.2–0.8 m in 0.1 m increments) and T (6–16 s in 2 s increments). The hydraulic conductivity was again set to $K = 10$ cm/s and simulations were carried out with

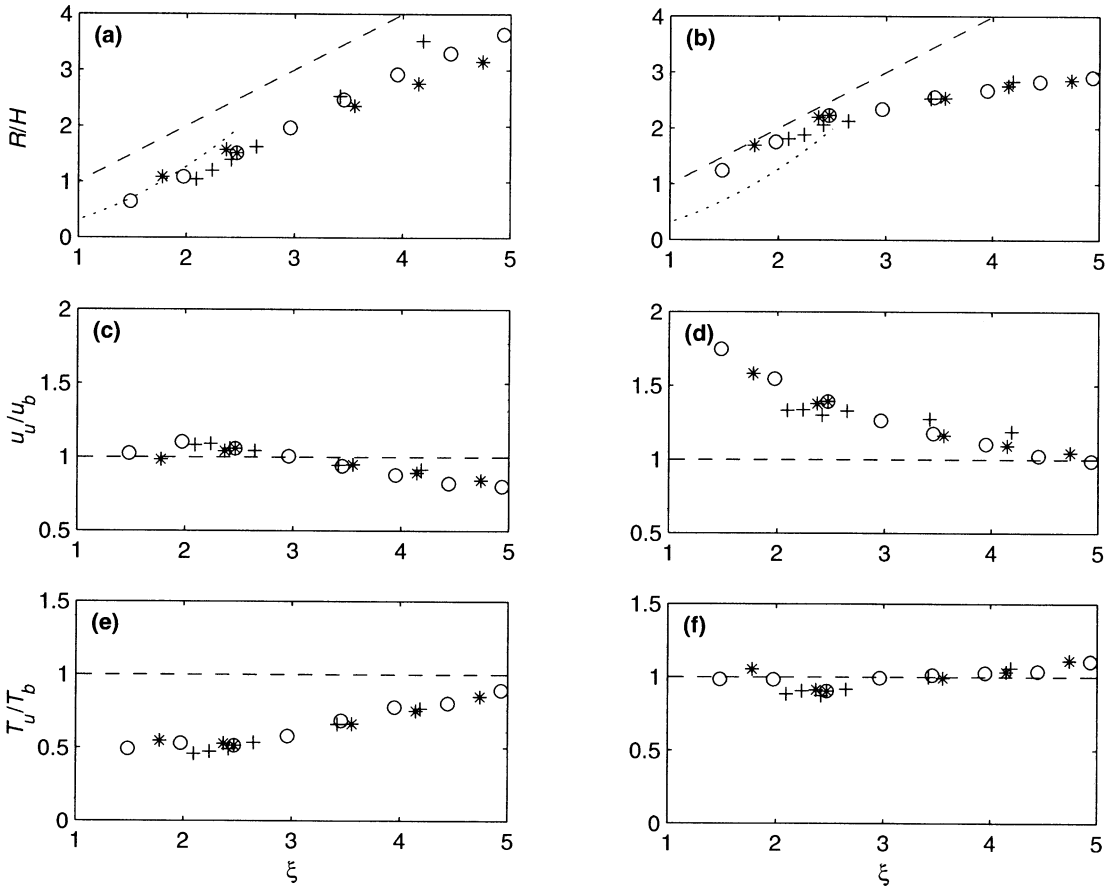

Fig. 6. Relationship between surf similarity parameter ξ and (a) normalized runup height R/H without groundwater effects; (b) R/H with groundwater effects; (c) swash velocity asymmetry u_u/u_b without groundwater effects; (d) u_u/u_b with groundwater effects; (e) time asymmetry T_u/T_b without groundwater effects; and (f) T_u/T_b with groundwater effects. The asymmetry values relate to the mid-swash zone position. A hydraulic conductivity of $K = 10$ cm/s was used. Symbols: (○) changes in beach gradient tan β; (+) changes in wave height H; and (∗) changes in wave period T.

and without groundwater effects. The following parameters were derived from the model output: (1) vertical swash excursion R normalized by the input wave height H; (2) velocity asymmetry u_u/u_b; and (3) time asymmetry T_u/T_b. The asymmetry parameters were determined for the mid-swash position ($x/S = 0.5$). The parameters derived from the swash records were plotted against the surf similarity parameter ξ

$$\xi = \frac{\tan\beta}{\sqrt{H/L_0}}, \tag{7}$$

where L_0 is the deep water wave length given by $gT^2/2\pi$ (Fig. 6).

As expected from the SWE (cf. Raubenheimer and Guza, 1996), R/H increases with ξ and plots around the curves predicted by the formula of Hunt (1959) ($R/H = \xi$) and saturated swash concept of Miche (1951) ($R/H = \xi^2/\pi$ for $\xi < 2$–3) (Fig. 6a, b). Thus, under dissipative (i.e. saturated conditions ($\xi < 2$), the vertical swash excursion zone is relatively small, whereas under reflective conditions ($\xi > 3$) the swash excursion is relatively large. Comparing the results of Fig. 6a and b, it is clear that swash infiltration has a significant effect on the wave runup. Under dissipative conditions, infiltration losses result in a lower backwash limit and hence larger R/H values. Under the reflective conditions, on the other hand, infiltration

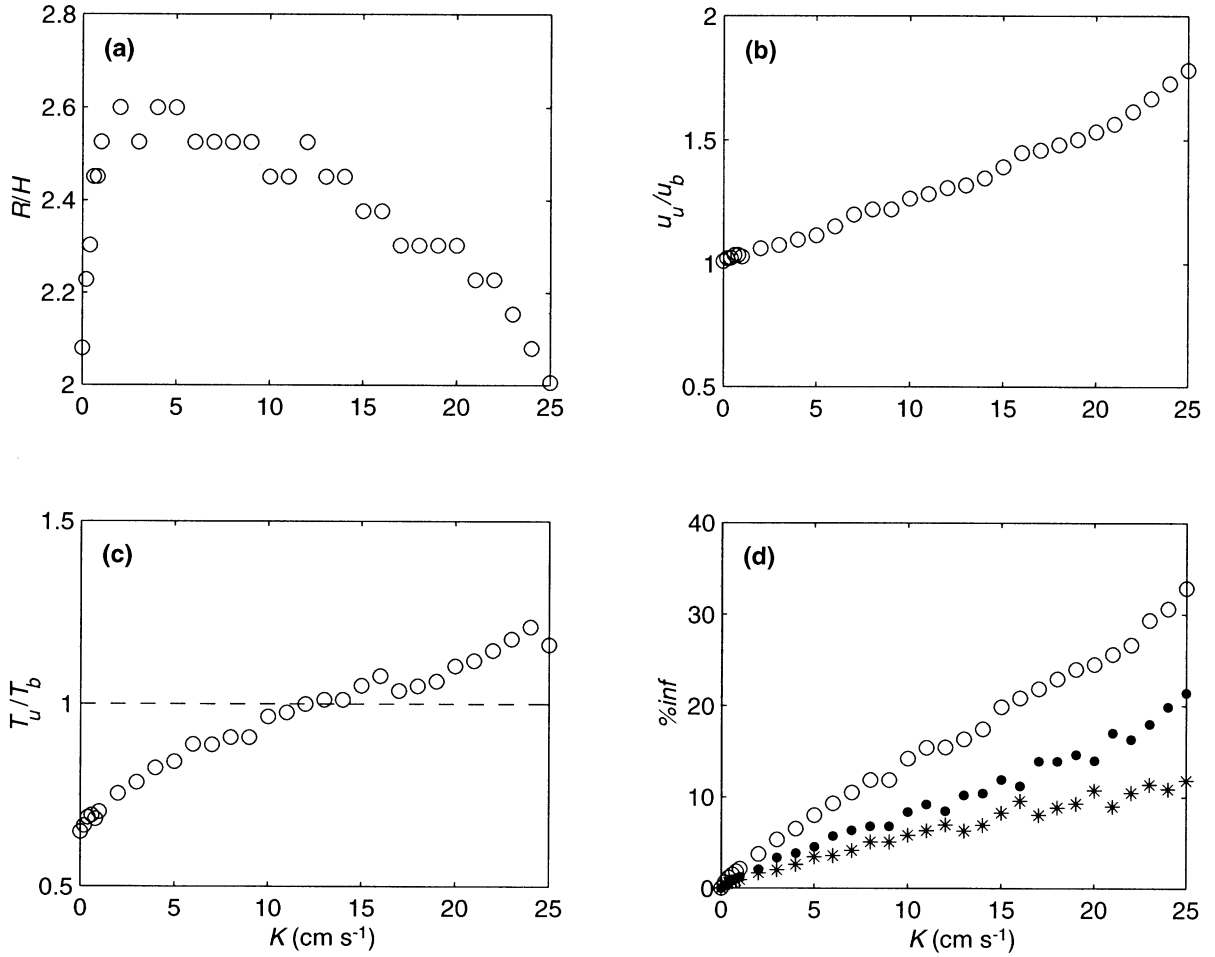

Fig. 7. Relationship between hydraulic conductivity K and (a) normalized runup height R/H; (b) velocity asymmetry u_u/u_b; (c) time asymmetry T_u/T_b; and (d) the percentage of uprush volume that infiltrates into the beach during swash motion *%inf*. Symbols in (d): (○) %inf over the complete swash cycle (uprush and backwash); (●) *%inf* during uprush; (*) *%inf* during backwash. The asymmetry values in (b) and (c) relate to the mid-swash zone position.

losses result in a lower runup limit and hence smaller R/H values.

When groundwater effects are ignored, the swash flow asymmetry u_u/u_b at the mid-swash position is around 1 over the entire morphodynamic domain (Fig. 6c) With groundwater effects accounted for, however, the swash flow is characterized by an onshore asymmetry ($u_u/u_b > 1$) that decreases with increasing ξ (Fig. 6d). If groundwater effects are ignored, the backwash period is considerably longer than the uprush period ($T_u/T_b < 1$) as long as $\xi < 5$ (Fig. 6e). As ξ approaches 5, the backwash period becomes shorter than the uprush period $T_u/T_b > 1$). In contrast, the results with groundwater effects show that $T_u/T_b \approx 1$ over both the dissipative and the reflective domain of ξ (Fig. 6f). It can be concluded that both flow and time asymmetry decrease with increasing ξ. This result is not unexpected because as flow conditions become reflective, swash motion develops into a standing wave, and if frictional and infiltration losses are ignored, the flow field associated with standing wave motion is symmetric. Such a symmetric swash motion is attained when $\xi \approx 5$. It is important to point out that

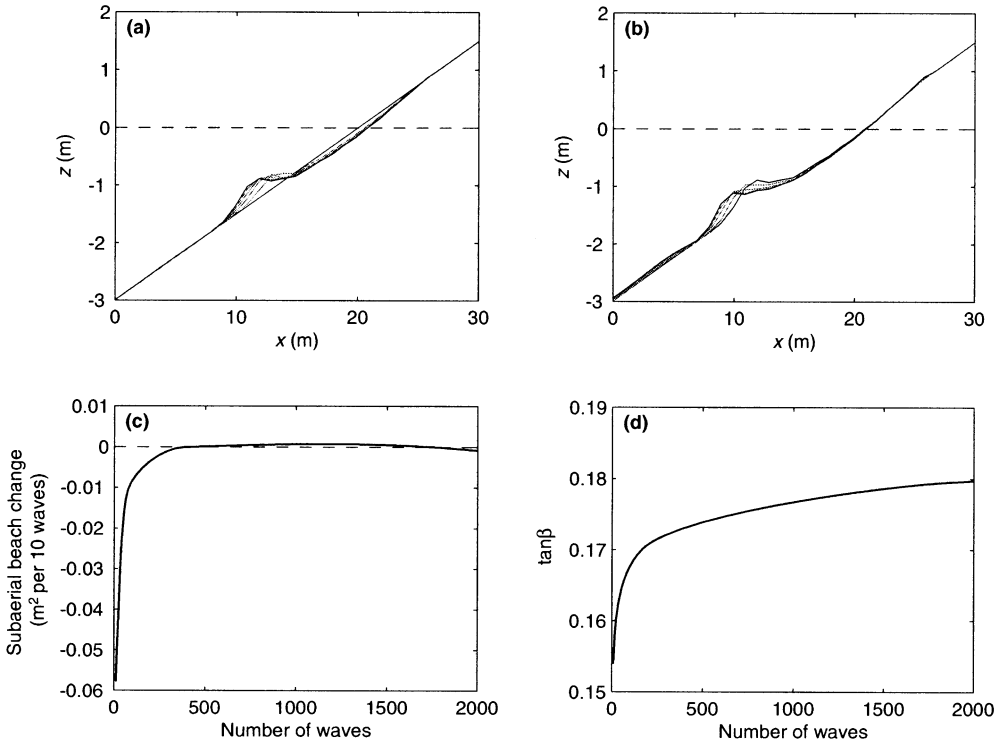

Fig. 8. Evolution of the beach profile for $H = 0.4$ m, $T = 10$ s, tan $\beta = 0.15$ and $K = 0$ cm/s: (a) beach profile at the start of the simulation and after 250 waves (black lines), and after 50, 100, 150 and 200 waves (gray lines); (b) beach profile after 250 waves and at the end of the simulation (black lines), and after 500, 750, 1000, 1250, 1500 and 1750 wave cycles (gray lines); (c) variation in subaerial beach volume; and (d) variation in swash zone gradient.

according to the modeling results, the flow asymmetry parameters, u_u/u_b and T_u/T_b, can be scaled reasonably well using ξ (Fig. 6c–f). In other words, a decrease in tan β has the same effect on the swash flow asymmetry as an increase in H or a decrease in T. Such scaling relation, which is physically meaningful and expected, gives added confidence to the model.

A further series of simulations were carried out to investigate the effect of hydraulic conductivity K on swash flow characteristics (Fig. 7). Model input conditions were tan $\beta = 0.15$, $H = 0.4$ m, $T = 10$ s and K varied from 0 (no groundwater effects) to 25 cm/s. Maximum R/H occurs for intermediate K-values ($K = 0.02$–0.06 cm/s; Fig. 7a). For less permeable sediments, the lowering of the downrush limit due to infiltration is limited, whereas for more permeable sediments the runup limit becomes significantly lower due to infiltration during wave uprush. Thus for both low and high K-values, R/H is relatively small. The velocity asymmetry of the swash flow u_u/u_b at the mid-swash position progressively increases from 1 to 1.8 with increasing hydraulic conductivity (Fig. 7b). For $K < 10$ cm/s, the time asymmetry of the swash flow T_u/T_b at the mid-swash position is smaller than one, indicating that the backwash is of longer duration than the uprush (Fig. 7c). On the other hand, T_u/T_b for $K > 10$ cm/s is larger than one, indicating that the uprush takes longer than the backwash.

The amount of water that infiltrates into the beach during swash motion was determined by integrating the groundwater flow (positive and negative) across the swash zone over one swash cycle. This value, representing the net groundwater discharge over one swash cycle, was related to the swash volume and expressed as a percentage *%inf*. An almost linear relationship exists between K and *%inf* (Fig. 7d). For small K-values, only a fraction of the swash volume infiltrates into the beach (e.g. for $K = 1$ cm/s,

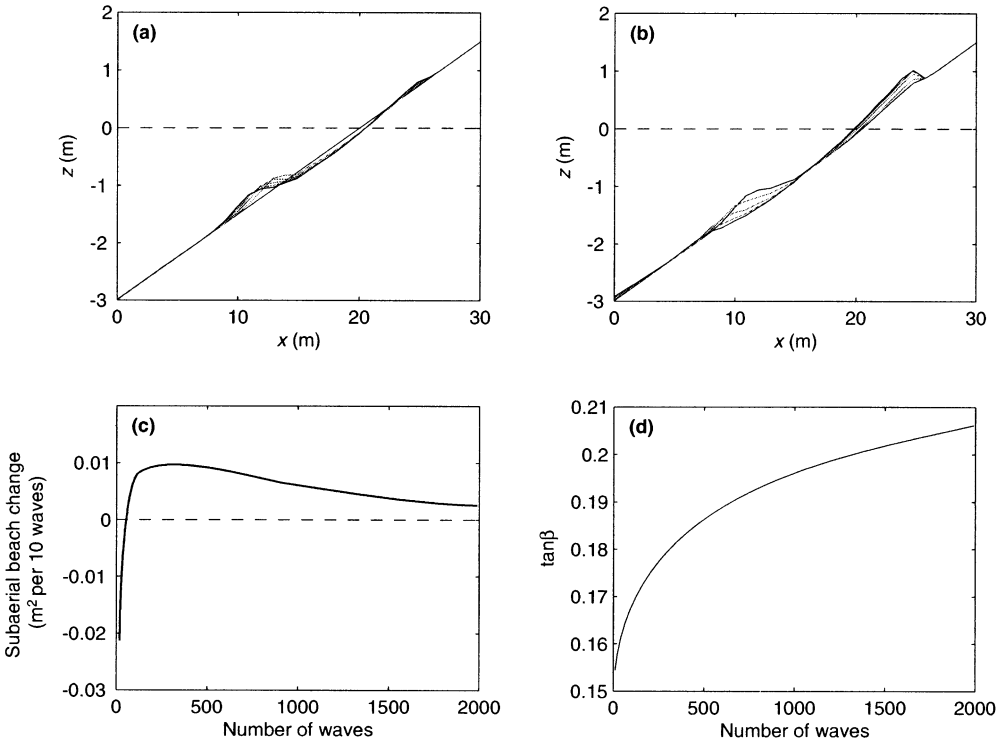

Fig. 9. Evolution of the beach profile for $H = 0.4$ m, $T = 10$ s, tan $\beta = 0.15$ and $K = 1.6$ cm/s: (a) beach profile at the start of the simulation and after 250 waves (black lines), and after 50, 100, 150 and 200 waves (gray lines); (b) beach profile after 250 waves and at the end of the simulation (black lines), and after 500, 750, 1000, 1250, 1500 and 1750 wave cycles (gray lines); (c) variation in subaerial beach volume; and (d) variation in swash zone gradient.

$\%inf = 2\%$), but for large K-values, a significant portion of the swash volume is lost through infiltration (e.g. for $K = 10$ cm/s, $\%inf = 15\%$). The majority of the infiltration loss occurs during wave uprush, but losses during backwash are also significant. It should be pointed out that the mass conservation principle requires that the infiltration volume equals the difference between the uprush volume and backwash volume. For all simulations, this was the case.

A series of simulations that included sediment transport and beach deformation were conducted to investigate the effect of swash infiltration on beach profile development. The simulations, based on standard wave conditions ($H = 0.4$ m and $T = 10$ s) and an initial beach gradient of 0.15, covered a range of values for hydraulic conductivity K. Each simulation was run for 2000 wave cycles (*c*. 6 h) to ensure that most of the beach deformation occurred within the simulation period and a quasi-equilibrium beach profile was attained for comparison.

Fig. 8 shows the model results for an impermeable beach ($K = 0$, i.e. groundwater effects are ignored). Beach profile development is characterized by sediment transfer from the subaerial to the subaquous beach, resulting in the formation of a distinct bar/step feature below the still water level and a steepening of the beachface. The initial response of the beach to the wave forcing is rapid and most of the profile adjustment is accomplished within the first 250 waves. Over the remainder of simulation the beachface is relatively stable, but the bar/step feature continues to move offshore, albeit at a progressively

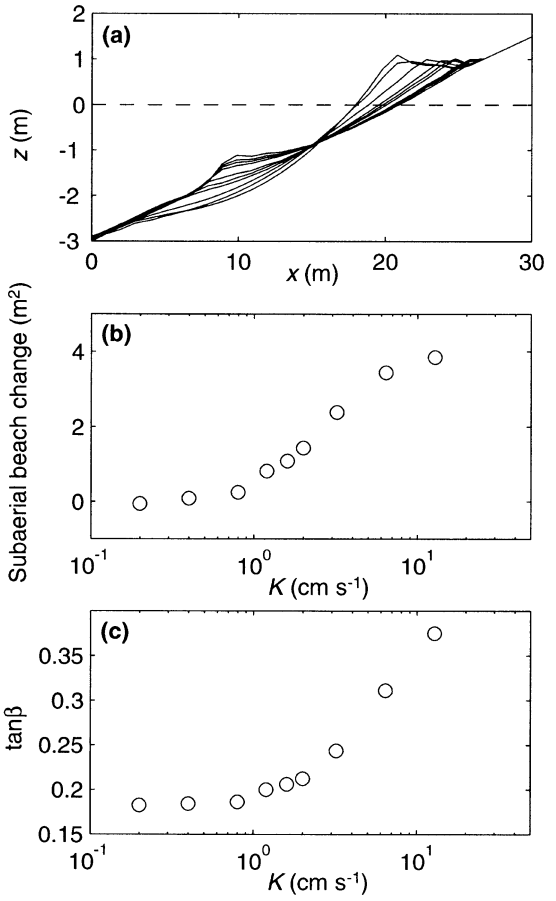

Fig. 10. Beach profile development for $H = 0.4$ m, $T = 10$ s, tan $\beta = 0.15$ and $K = 0$, 0.2, 0.4, 0.8, 1.2, 1.6, 2, 3.2 and 6.4 cm/s from simulations over 2000 wave cycles: (a) beach profiles at the end of the simulation; (b) relation between subaerial beach volume at the end of the simulation (surrogate for berm size) and K; and (c) relation between swash zone gradient at the end of the simulation and K. All beach profiles have been superimposed in (a), but are easily identifiable because the size of the berm is positively related to K and the size of the step is negatively related to K. The results for $K = 0$ are not plotted in (b) and (c) due to the logarithmic x-axis.

reducing pace. A quasi-equilibrium is reached at the end of the simulation.

The beachface erosion at the start of the simulation occurs because the swash zone processes encounter a gradient that is too steep. As a result, the offshore sediment transport during the backwash exceeds that of the uprush causing beachface erosion. The combing down of the beachface results in a steepening of the gradient, not a flattening as suggested by previous morphodynamic models (Hardisty, 1984). The concurrence of beachface erosion and steepening seems at a first glance contradictory. However, morphological change results from spatial gradients in sediment transport and is not achieved by a profile-wide tendency to flatten or steepen. On the initially planar beachface offshore sediment transport prevails because the backwash is more powerful than the uprush. Because the offshore sediment transport rate increases down the beach from the runup limit to the downrush limit, more sediment is removed from the lower part of the swash zone than the upper part. The only outcome of such a sediment transport pattern is a steepening of the beachface (i.e. the gradient increases). Equilibrium is attained at some stage because as the gradient in the swash zone becomes steeper, the swash motion becomes more symmetrical (refer to Fig. 6).

The model results for a relatively permeable beach $K = 1.6$ cm/s (equivalent to fine gravel) are shown in Fig. 9. Beach development is characterized by initial beachface erosion and the development of a bar/step feature, but this is quickly followed by onshore sediment transport and the formation of a berm. As the berm builds up, the gradient of the swash zone progressively increases and attains a relatively stable value of 0.21 at the end of the simulation. It is noted that when groundwater effects are ignored, the model produces an equilibrium beach profile relatively rapidly, but when groundwater effects are included it takes a very long time before equilibrium is established.

When comparing Fig. 8 with Fig. 9 it is clear that swash infiltration enhances onshore sediment transport in the swash zone resulting in the formation of a berm. In addition, the quasi-equilibrium gradient in the swash zone is greater when swash infiltration occurs. Simulations were also conducted with lower and higher K to examine the effects of sediment permeability on the beach morphology. The results show that the subaerial beach volume (a measure of the size of the berm and hence the amount of onshore sediment transport in the swash zone) and the equilibrium gradient in the swash zone are both positively related to the hydraulic conductivity K (Fig. 10). The relation between the beach morphology and K is, however, highly non-linear. Up to $K = 1$ cm/s, the effect of permeability is negligible. Once K is larger

than this thereshold value, permeability greatly affects beach profile development.

The results of the numerical model highlight the role of swash infiltration in controlling the equilibrium beachface gradient by influencing swash dynamics and hence sediment transport. The numerical results firmly substantiate the claim that swash acting on beaches with coarse sediments produces steeper gradients than on beaches with fine sediments due to enhanced swash infiltration as first suggested by Grant (1948). Infiltration of water into the beach occurs primarily during the wave uprush, whereas exfiltration of water out of the beach mainly occurs during the backwash. The net water circulation is characterized by net infiltration over the swash zone and net exfiltration seaward of the swash zone (Longuet-Higgins, 1983; Li and Barry, 2000). The effect of swash infiltration is mainly to reduce the duration and velocity of the backwash flow; the uprush phase of the swash is not much affected. This results in an increase in the onshore flow asymmetry and promotes onshore sediment transport and the development of steeper equilibrium gradient results.

According to the numerical model, the effect of swash infiltration on beachface gradient is only important when the permeability K exceeds 1 cm/s. For lower values of K, swash infiltration still occurs, but the quantities involved are too small to significantly affect the swash hydrodynamics (less than *c.* 2% of the wave uprush volume; refer to Fig. 7). It is informative to relate this threshold value for K to sediment size. The Hazen equation is one of the most commonly used equations and is given by $K = 0.01D_{10}^2$ where K is in m/s and D_{10} is in mm (Bear, 1972). For well-sorted sediments, such as beach sediment, $D_{50} \approx 1.5D_{10}$ and the Hazen equation becomes $K = 0.0044D_{50}^2$. Application of this formulation suggests that the threshold hydraulic conductivity of $K = 1$ cm/s that has emerged from the present work corresponds to a sediment size of c. 1.5 mm. Beach sediments are generally very well sorted and rounded. Both factors would significantly enhance the permeability. However, it is not known how well the permeability of beach sediments is predicted by the Hazen equation. To the authors' knowledge, Hegge (1994) is the only study that reports in situ measurements of permeability on a number of beaches (refer to Fig. 2). Least-squares analysis of the results of Hegge, 1994 results yielded $K = 0.0062D_{50}^2$ ($r^2 = 0.50$; $N = 33$) and application of this formula gives a threshold sediment size of 1.27 mm which is in reasonable agreement with the Hazen equation.

The present study focuses on swash asymmetry induced/enhanced by infiltration (i.e. swash infiltration losses) and the results indicate that the effect of swash infiltration on sediment transport in the swash zone is insignificant for sandy beaches. However, this does not imply that vertical flows through the beachface due to instantaneous in-exfiltration are not important. The implications for swash zone sediment transport of infiltration under wave uprush and exfiltration under backwash have been investigated for a saturated beach face by Turner and Masselink (1998). Vertical flow through a porous bed can affect sediment mobility in two ways: (1) seepage forces change the effective weight of surficial sediments (Martin and Aral, 1971); and (2) boundary layer thinning due to infiltration or thickening due to exfiltration result in altered bed shear stresses (Conley and Inman, 1994). Recently, Butt et al. (2001) hypothesized that there is a threshold grain size where the dominance goes from stabilization–destabilization (promoting offshore transport) to boundary layer modification (promoting onshore transport), and that this critical grain size is 0.24 mm. The present paper suggests the presence of a second critical grain size of 1.5 mm above which swash infiltration losses, also promoting onshore transport, start playing a significant role.

Numerous empirical studies clearly demonstrate that the beachface gradient is closely related to the sediment size even within the sand fraction (e.g. Bascom, 1951; Shepard, 1963). The present results demonstrate, however, that the increase in beachface gradient as a function of sediment size as found on sandy beaches can not be attributed to changes in the asymmetry of the swash flow due to swash infiltration because the amount of swash infiltration on these beaches is not sufficient to significantly modify the characteristics of the swash flow. Komar (1998) suggested there are two types of sediment transport regimes in the swash zone. On fine-grained beaches, beachface morphology is controlled by suspended

sediment processes and the equilibrium gradient is related to the sediment fall velocity. On coarse-grained beaches, sediment dynamic conditions on the beachface are controlled by swash flow asymmetry due to swash infiltration and the equilibrium gradient is related to the permeability. This study suggests that the latter sediment transport regime occurs when $D_{50} > 1.5$ mm.

The sediment transport equations incorporated in the numerical model are supposed to display self-stabilizing characteristics through the inclusion of the beach gradient, whereby any perturbation from the equilibrium induces a response which opposes the change and returns the beach toward the equilibrium condition (Hardisty, 1984; Jago and Hardisty, 1984). However, it appears that the swash zone morphodynamic system is quite unstable when subjected to erosive wave conditions because its response to an over-steepened bed is to steepen even more. Nevertheless, at some stage the swash zone morphology becomes quasi-stable and the equilibrium gradient can be determined. Equilibrium is the product of negative feedback and in the present numerical model this is represented by the fact that the time asymmetry of the swash motion decreases with increasing bed gradient. Ignoring swash infiltration, the motion of the swash on a steep gradient under reflective conditions resembles that of standing wave whereby $u_u \approx u_b$ and $T_u \approx T_b$ (refer to Fig. 5). Subsequently, the equilibrium gradient becomes simply a function of the ratio k_u/k_b:

$$\tan \beta = \tan \phi \frac{k_u/k_b - 1}{k_u/k_b + 1}. \quad (8)$$

For k_u/k_b is 2, as assumed in the present study, the equilibrium beachface gradient becomes $\tan \beta = 0.21$ which is in reasonably agreement with the model results.

In the simulations, the water table elevation at the landward boundary (100 m from the shore) was set to be the same as the mean sea level. On natural beaches affected by tides, the position of the landward water table relative to the mean sea level varies with the tidal stages. At high tide, the water table becomes relatively low, whereas the opposite occurs during low tide. Although swash infiltration is a localized phenomenon mainly driven by the hydraulic gradients created by wave motion, it is also affected by the landward hydraulic conditions (Li and Barry, 2000). Swash infiltration is likely to increase at high tide and decrease at low tide. Due to the non-linear nature of the swash infiltration effects as shown in Fig. 10b, c, tidal influence may result in a further increase in the beachface gradient. Other factors that have not been considered in the present study but may affect swash infiltration include the randomness of the wave field and beach dewatering. Under random waves, large wave runup may occur on the dry bed, leading to increased infiltration. Beach dewatering aims to lower the water table and induces high infiltration rates. Therefore, it is likely that the results presented here represent the minimum effects of groundwater flow on the beach morphology.

Swash infiltration increases the asymmetry in the swash flow by reducing the backwash strength and duration. The increased swash asymmetry enhances on-shore sediment transport and berm formation, resulting in relatively steep beachface gradients. The effects of swash infiltration are highly non-linear. Swash infiltration affects the beach morphology only if the total infiltration volume over a wave cycle exceeds c. 2% of the uprush volume. This threshold condition leads to two critical parameters: critical sediment hydraulic conductivity $K = 1$ cm/s and grain size $D_{50} = 1.5$ mm. Therefore, swash infiltration has negligible effects on sandy beaches where the sediment grain size is usually less than 1 mm. The correlation between the beachface gradient and sediment size at these beaches is due to other mechanisms, rather than swash infiltration. For gravel beaches, however, swash infiltration is likely to be the dominant factor in controlling the beachface gradient.

We would like to thank Bruce Hegge for providing the data plotted in Fig. 2. Paul Russell and an anonymous reviewer provided useful comments on the manuscript.

Bagnold, R.A., 1940. Beach formation by waves: some model experiments in a wave tank. J. Inst. Civil Engrs. 15, 27–52.

Bagnold, R.A., 1963. Mechanics of marine sedimentation. In: Hill, M.N. (Ed.), The Sea, vol. 3. Wiley-Interscience, New York, pp. 507–528.

Bagnold, R.A., 1966. An approach to the sediment transport problem from general physics. Geol. Surv. Prof. Pap. 422-I, 37.

Baird, A.J., Horn, D., Mason, T., 1996. Mechanisms of beach ground-water and swash interaction. 25th Int. Conf. Coastal Engng, ASCE, 4120–4133.

Bascom, W.N., 1951. The relationship between sand size and beach-face slope. Trans. Am. Geophys. Union 32, 866–874.

Bear, J., 1972. Dynamics of Fluids in Porous Media. American Elsevier, New York, p. 764.

Butt, T., Russell, P., 2000. Hydrodynamics and cross-shore sediment transport in the swash zone of natural beaches: a review. J. Coast. Res. 16, 255–268.

Butt, T., Russell, P., Turner, I., 2001. The influence of swash infiltration–exfiltration on beach face sediment transport: onshore or offshore? Coast. Engng 42, 35–52.

Conley, D.C., Inman, D.L., 1994. Ventilated oscillatory boundary layers. J. Fluid Mech. 273, 261–284.

Dalrymple, R.A., Thompson, W.W., 1976. Study of equilibrium profiles. Proc. 15th Int. Conf. Coast. Engng, 1277–1296.

Dean, R.G., 1973. Heuristic models of sand transport in the surf zone. Proc.Conf. Engng Dyn. Surf Zone, ASCE, 208–214.

Dubois, R.N., 1972. Inverse relation between foreshore slope and mean grain size as a function of the heavy mineral content. Geol. Soc. Am. Bull. 83, 871–876.

Edwards, A., 1997. Sediment transport in the swash zone of a sandy beach. Honours Thesis (unpublished). University of Western Australia, Perth, p. 153.

Grant, U.S., 1948. Influence of the water table on beach aggradation and degradation. J. Mar. Res. 7, 655–660.

Hardisty, J., 1984. A morphodynamic model for beach gradients. Earth Surf. Processes Landforms 11, 327–333.

Hegge, B.J., 1994. Low-energy sandy beaches of southwestern Australia: Two-dimensional morphology and dynamics. PhD Thesis (unpublished). University of Western Australia, Perth, p. 419.

Hughes, M.G., Masselink, G., Brander, R.W., 1997. Flow velocity and sediment transport in the swash zone of a steep beach. Mar. Geol. 138, 91–103.

Hunt, L.A., 1959. Design of seawalls and breakwaters. Proc. Am. Soc. Civil Engrs. 85, 123–152.

Jago, C.F., Hardisty, J., 1984. Sedimentology and morphodynamics of a macrotidal beach, Pendine Sands, SW Wales. Mar. Geol. 60, 123–154.

Kemp, P.H., 1975. Wave asymmetry in the nearshore zone and breaker area. In: Hails, J., Carr, A. (Eds.), Nearshore Sediment Dynamics and Sedimentation. Wiley, London, pp. 47–67.

King, D.B., 1991. Studies in oscillatory flow bedload sediment transport. PhD Thesis (unpublished). University of California, San Diego, p. 183.

Kobayashi, N., DeSilva, G.S., Watson, K.D., 1989. Wave transformation and swash oscillation on gentle and steep slopes. J. Geophys. Res. 94, 951–966.

Komar, P.D., 1998. Beach Processes and Sedimentation. second ed.. Prentice-Hall, New Jersey, p. 544.

Krumbein, W.C., Monk, G.D., 1942. Permeability as a function of the size parameters of unconsolidated sand. American Institute of Mining and Metallurgical Engineering, Technical Publication 1492, p. 11.

Li, L., Barry, D.A., 2000. Wave-induced beach groundwater flow. Adv. Water Resour. 23, 325–337.

Li, L., Barry, D.A., Parlange, J.-Y., Pattiaratchi, C.B., 1997. Beach water table fluctuations due to wave runup: Capillarity effects. Water Resour. Res. 33, 935–945.

Li, L., Barry, D.A., Pattiaratchi, C.B., Masselink, G., 2001. BeachWin: modelling groundwater effects on swash sediment transport and beach profile changes. Environmental Modelling and Software, submitted.

Longuet-Higgins, M.S., 1983. Wave set-up, percolation and undertow in the surf zone. Proc. R. Soc. London Ser. A390, 283–291.

Makaske, B., Augustinus, P.G.E.F., 1998. Morphologic changes of a micro-tidal, low wave energy beach face during a spring-neap tidal cycle, Rhone Delta, France. J. Coast. Res. 14, 632–645.

Martin, C.S., Aral, M.M., 1971. Seepage force on interfacial bed particles. J. Hydraul. Div. 7, 1081–1100.

Masselink, G., Hughes, M.G., 1998. Field investigation of sediment transport in the swash zone. Continental Shelf Res. 18, 1179–1199.

McLean, R.F., Kirk, R.M., 1969. Relationship between grain size, size-sorting, and fore-shore slope on mixed sand-shingle beaches. New Zealand J. Geol. Geophys. 12, 138–155.

Miche, R., 1951. Le pouvoir réfléchissant des ouvrages maritimes exposés a l'action de la houle. Ann. Ponts Chaussees 121, 285–319.

Nielsen, P., 1992. Coastal Bottom Boundary Layers and Sediment Transport. Advanced Series on Ocean Engineering, 4. World Scientific, Singapore, p. 324.

Packwood, A.R., Peregrine, D.H., 1979. The propagation of solitary waves and bores over porous bed. Coast. Engng 3, 221–242.

Packwood, A.R., Peregrine, D.H., 1981. Surf and run-up on beaches: models of viscous effects. Technical Report AM-81-07, University of Bristol, UK.

Parlange, J.-Y., Brutsaert, W., 1987. A capillary correction for the free surface flow of groundwater. Water Resour. Res. 23, 805–808.

Peregrine, D.H., 1972. Equations for water waves and the approximations behind them. In: Meyer, R.E. (Ed.), Waves on Beaches and Resulting Sediment Transport. Academic Press, New York.

Puleo, J.A., Beach, R.A., Holman, R.A., Allen, J.S., 2000. Swash zone sediment suspension and transport and the importance of bore-generated turbulence. J. Geophys. Res. 105, 17021–17044.

Quick, M.C., 1991. Onshore-offshore sediment transport on beaches. Coastal Engng 15, 313–332.

Raubenheimer, B., Guza, R.T., 1996. Observations and predictions of run-up. J. Geophys. Res. 101, 25575–25587.

Ribberink, J.S., Al Salem, A., 1990. Bed forms, sediment

concentrations and sediment transport in simulated wave conditions. Proc. 22nd Int. Conf. Coast. Engng, ASCE, 2318–2331.
Shepard, F., 1963. Submarine Geology. 3rd ed. Harper and Row, New York.
Sonu, C.J., van Beek, J.L., 1971. Systematic beach changes on the Outer Banks, North Carolina. J. Geol. 79, 416–425.
Sonu, C.J., James, W.R., 1973. A Markov model for beach profile changes. J. Geophys. Res. 78, 1462–1471.
Sunamura, T., 1984. Quantitative predictions of beach-face slopes. Geol. Soc. Am. Bull. 95, 242–245.
Turner, I., 1993. Water table outcropping on macro-tidal beaches: A simulation model. Mar. Geol. 115, 227–238.
Turner, I.L., Leatherman, S.P., 1997. Beach dewatering as a soft engineering solution: a history and critical review. J. Coast. Res. 13, 1050–1063.
Turner, I.L., Masselink, G., 1998. Swash infiltration–exfiltration and sediment transport. J. Geophys. Res. 103, 30813–30824.
Wilson, K.C., 1987. Analysis of bed-load motion at high shear stress. J. Hydraul. Engng 113, 97–103.